Importance of anisotropy in the spin-liquid candidate $Me_3EtSb[Pd(dmit)_2]_2$

A. C. Jacko, Luca F. Tocchio, Harald O. Jeschke, and Roser Valentí
Institut für Theoretische Physik, Goethe-Universität Frankfurt, Max-von-Laue-Straße 1, 60438 Frankfurt am Main, Germany
(Received 19 August 2013; published 31 October 2013)

Organic charge-transfer salts based on the molecule $Pd(dmit)_2$ display strong electronic correlations and geometrical frustration, leading to spin-liquid, valence bond solid, and superconducting states, among other interesting phases. The low-energy electronic degrees of freedom of these materials are often described by a single band model: a triangular lattice with a molecular orbital representing a $Pd(dmit)_2$ dimer on each site. We use *ab initio* electronic structure calculations to construct and parametrize low-energy effective model Hamiltonians for a class of Me_{4-n} $Et_nX[Pd(dmit)_2]_2$ (X = As, P, N, Sb) salts and investigate how best to model these systems by using variational Monte Carlo simulations. Our findings suggest that the prevailing model of these systems as a $t-t'$ triangular lattice is incomplete and that a fully anisotropic triangular lattice description produces importantly different results, including a significant lowering of the critical U of the spin-liquid phase.

DOI: 10.1103/PhysRevB.88.155139 PACS number(s): 71.15.Mb, 71.10.Fd, 71.20.−b

I. INTRODUCTION

The $Me_{4-n}Et_nX[Pd(dmit)_2]_2$ family of organic crystals[1] is known for its many interesting electronic and magnetic phases; these materials can have superconducting, Mott insulating, spin-liquid, valence bond solid, and spin-density wave orders, determined by the cation as well as by temperature and applied pressure.[2–5] The reason for this rich variety of phases is the competition between frustration effects and electronic correlations. As such, these materials are the focus of very active research. Here we will investigate the significance of anisotropy and correlations in these materials by parametrizing and solving model Hamiltonians. We will abbreviate $Me_{4-n}Et_nX[Pd(dmit)_2]_2$ as X-n, following Ref. 6.

These materials share a generic crystal structure, illustrated in Fig. 1, and are found in a variety of ordered phases.

As-0 enters an antiferromagnetic (AFM) phase below 35 K; Sb-1 has a spin-liquid ground state, and spin susceptibility measurements imply that it has an exchange interaction $220 \leqslant J \leqslant 250$ K; Sb-2 has no low-temperature AFM transition (unlike P-2 and most of the X-0s); N-0 is the only X-0 material with a superconducting transition (6.2 K at 6.5 kbars), while at lower pressures (away from the superconducting phase) it exhibits a spin-density wave transition.[2–5] Developing a unified description of this wide variety of phases is an ongoing challenge.

Here we calculate the electronic structure and use Wannier orbitals for the frontier bands to parametrize model Hubbard Hamiltonians. By solving these Hamiltonians with variational Monte Carlo (VMC), we show that there are important qualitative differences between treating the system as a $t-t'$ triangular lattice and considering it as a fully anisotropic triangular lattice (FATL). A discussion on the role of full anisotropy within the Heisenberg model may be found in Ref. 7.

II. METHODS

We perform density-functional theory calculations of the electronic structure and then construct localized Wannier orbitals for the frontier bands. From these we parametrize tight-binding model Hamiltonians, both for the $t-t'$ and for the FATL ($t_a - t_b - t_c$). We then solve these models with a VMC approach. The approach used here allows for the description of metallic and spin-liquid states with the same variational wave function, which is compared to a variational wave function that describes the magnetic spiral ordered insulating state.

A. Electronic structure

The electronic structure calculations presented here were performed in an all-electron full-potential local-orbital basis using the FPLO package.[8] The densities were converged on a $(6 \times 6 \times 6)$ k mesh using a generalized gradient approximation functional.[9]

To move from density-functional theory calculations to model Hamiltonians, it is convenient to construct Wannier orbitals to represent the frontier bands of the system. In principle the Wannier orbitals are simply Fourier transforms of the Bloch wave functions; however, in this procedure there are still many degrees of freedom. Here they are constrained by the requirements that the Wannier orbitals be represented by Kohn-Sham orbitals in a narrow energy window; projecting onto the FPLO basis orbitals ensures that they will form a good basis for a tight-binding model.[10] With these nearly optimally localized Wannier orbitals we compute real-space overlaps to obtain tight-binding parameters. This method has several advantages over band fitting, as has been discussed previously in the case of molecular organic crystals.[11]

B. Effective modeling

To model these systems we consider the Hubbard Hamiltonian. As we will show later, a half-filled single orbital per site Hubbard model is suggested by the electronic structure, so it is this kind of model we will focus on. The Hamiltonian is defined by

$$\mathcal{H} = -\sum_{i,j,\sigma} t_{ij} c^{\dagger}_{i,\sigma} c_{j,\sigma} + U \sum_{i} n_{i,\uparrow} n_{i,\downarrow}, \qquad (1)$$

where $c^{\dagger}_{i,\sigma}(c_{i,\sigma})$ creates (destroys) an electron with spin σ on site i, $n_{i,\sigma} = c^{\dagger}_{i,\sigma} c_{i,\sigma}$ is the electronic density, t_{ij} is the hopping amplitude, and U is the on-site Coulomb repulsion. Here we

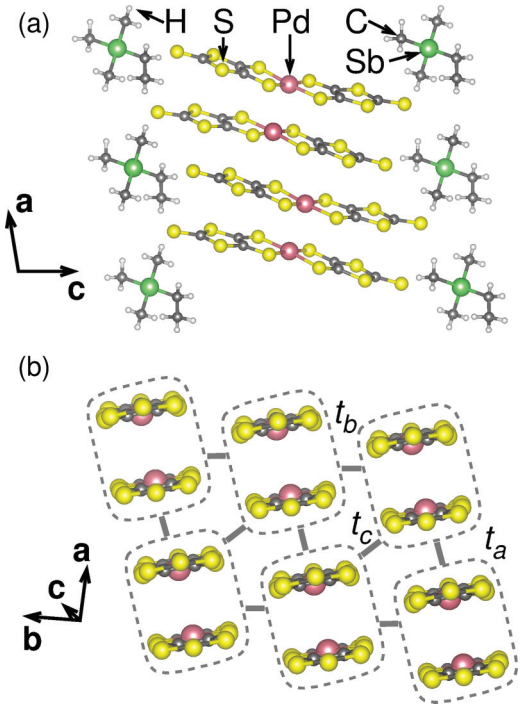

FIG. 1. (Color online) (a) Structure of the spin-liquid candidate $Me_3EtSb[Pd(dmit)_2]_2$ (Sb-1). (b) Dimerization of the $Pd(dmit)_2$ molecules, where dimers form 2D triangular lattice layers in the a-b plane, separated along c by cation layers (in this case, Me_3EtSb). We follow Ref. 21 in labeling the hopping integrals in the a-b plane t_a, t_b, and t_c.

calculate a VMC solution including backflow correlations, which allows us to provide an accurate description of a system with hundreds of lattice sites.[12]

A major issue in the Hubbard model on the anisotropic triangular lattice is the possibility of stabilizing a spin-liquid phase (as seen in the experimental data). In addition, for generic values of the hopping parameters magnetic states with generic spiral order may be expected and indeed can be obtained within mean-field approaches, like for instance the Hartree-Fock (HF) approximation.[13,14]

Here, we approach this problem by implementing correlated variational wave functions which describe both spin-liquid states and magnetic states with generic ordering vectors. In this way, we are able to treat spiral order and paramagnetic states at the same level of theory and therefore have a sensible comparison of their energies versus U.[15]

1. Spiral magnetic states

We start with the magnetic states obtained at the HF level, with the only constraint being that the spin order must be coplanar in the x-y plane. Our magnetic HF solutions display spiral order, which (in two dimensions) may be parametrized by two pitch angles θ and θ', where θ (θ') is the angle between nearest-neighbor spins along the hopping direction t_b (t_c). Since we use finite clusters, only certain commensurate angles are allowed. For a lattice size $L = l \times l$, the allowed values are $\theta = 2\pi n/l$ and $\theta' = 2\pi n'/l$, with n and n' being integers. We tested various lattice sizes ranging from 12×12 to 20×20 and determined the best pair of pitch angles for each lattice size.

Our VMC magnetic states are then constructed by applying correlation terms on top of the HF spiral states $|\mathrm{SP}\rangle$. We employ a spin-spin Jastrow factor to correctly describe fluctuations orthogonal to the plane where the magnetic order lies, i.e., $\mathcal{J}_s = \exp[\frac{1}{2}\sum_{i,j} u_{i,j} S^z_i S^z_j]$.[16] A further density-density Jastrow factor $\mathcal{J}_c = \exp[\frac{1}{2}\sum_{i,j} v_{i,j} n_i n_j]$ (that includes the on-site Gutzwiller term $v_{i,i}$) is considered to adjust electron correlations. All the $u_{i,j}$ and the $v_{i,j}$ are optimized for each independent distance $|i - j|$. The correlated state is then given by $|\Psi_{\mathrm{SP}}\rangle = \mathcal{J}_s\mathcal{J}_c|\mathrm{SP}\rangle$.

2. Paramagnetic states

In order to describe a paramagnetic state, we construct an uncorrelated wave function given by the ground state $|\mathrm{BCS}\rangle$ of a superconducting BCS Hamiltonian:[17,18]

$$\mathcal{H}_{\mathrm{BCS}} = \sum_{i,j,\sigma} \tilde{t}_{ij} c^\dagger_{i,\sigma} c_{j,\sigma} - \mu \sum_{i,\sigma} c^\dagger_{i,\sigma} c_{i,\sigma} + \sum_{i,j} \Delta_{ij} c^\dagger_{i,\uparrow} c^\dagger_{j,\downarrow} + \mathrm{H.c.}, \quad (2)$$

where both the variational hopping amplitudes $\tilde{t}_{ij}$, the pairing fields Δ_{ij}, and the chemical potential μ are variational parameters to be independently optimized. For the majority of the results reported here we constrain all of these variational parameters to be real.

The correlated state $|\Psi_{\mathrm{BCS}}\rangle = \mathcal{J}_c|\mathrm{BCS}\rangle$ allows us to describe a paramagnetic Mott insulator for a sufficiently singular Jastrow factor $v_q \sim 1/q^2$ (v_q being the Fourier transform of $v_{i,j}$),[19] while a metallic state can be obtained whenever $v_q \sim 1/q$.

A size-consistent and efficient way to further improve the correlated states $|\Psi_{\mathrm{BCS}}\rangle$ and $|\Psi_{\mathrm{SP}}\rangle$ is based on backflow correlations. In this approach, each orbital that defines the unprojected states $|\mathrm{BCS}\rangle$ and $|\mathrm{SP}\rangle$ is taken to depend upon the many-body configuration, in order to incorporate virtual hopping processes.[12] All results presented here are obtained by fully incorporating the backflow corrections and optimizing individually every variational parameter in the mean-field BCS equation, in the Jastrow factors $\mathcal{J}_c$ and $\mathcal{J}_s$, as well as in the backflow corrections.

III. DETERMINATION OF AN APPROPRIATE MODEL

The spin-liquid candidate Sb-1 has been the subject of much recent study. We will focus on this material in discussing the process of determining the appropriate model Hamiltonian for this class of systems. To move toward the goal of understanding the phase diagram of Sb-1, and the origin of the various ordered phases, one needs a sensible choice of a model Hamiltonian with reliable parameters. In constructing some minimal model, one must also be aware of what the model neglects and what effect that has on the physics it predicts. Here we analyze the electronic structure to determine an appropriate minimal model and then use Wannier orbitals to parametrize it.

Figure 2 shows the band structure and the density of states for Sb-1 in a wide energy window around the Fermi energy. From this figure, we can see that there are several pairs of bands

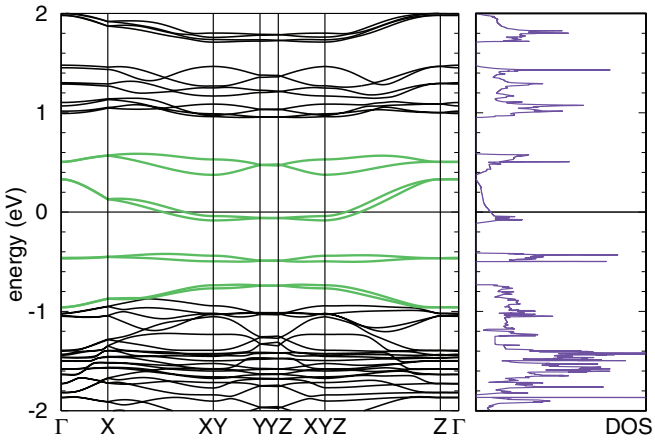

FIG. 2. (Color online) Band structure and density of states of Sb-1 in a wide energy window around the Fermi energy. The four pairs of bands highlighted in green are those identified as being of $Pd(dmit)_2$ HOMO or LUMO origin. The pair that crosses the Fermi energy is of HOMO-ab origin. These are the bands used in a minimal one-orbital model of the system. The direct energy gap between the HOMO-ab bands and the others is more than 0.1 eV, although the indirect gap is smaller.

separated from the others; these bands are the bands identified as arising from bonding (-b) and antibonding (-ab) hybrids of $Pd(dmit)_2$ highest occupied molecular orbitals (HOMO) and lowest unoccupied molecular orbitals (LUMO) (highlighted in green). The pair crossing the Fermi energy are HOMO-ab bands, while the pairs on either side are the LUMO-b and -ab bands. The fourth highlighted pair at the top of the bulk valence bands is the HOMO-b pair. The origin of these bands is illustrated in Fig. 3. The bands come in pairs because for each dimer orbital in one plane there is an identical one in the other plane, related to the first by a translation and a rotation about the t_b direction (the y axis). These pairs of bands are well separated from each other, with typical direct band gaps on the order of hundreds of meV, well above $k_B T$ for most experiments on these systems.

A. Modeling the frontier bands

As Fig. 2 shows, the HOMO-ab bands are well separated from the other bands, and so they form a good basis for a low-energy effective model Hamiltonian. In Fig. 4 we

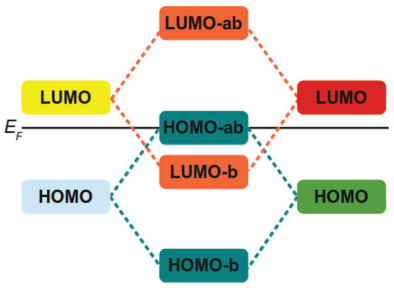

FIG. 3. (Color online) Schematic of the hybridization of the orbital of the two $Pd(dmit)_2$ in each dimer and the resultant crossing of energy levels leading to the unusually ordered frontier bands of $Pd(dmit)_2$ complexes.

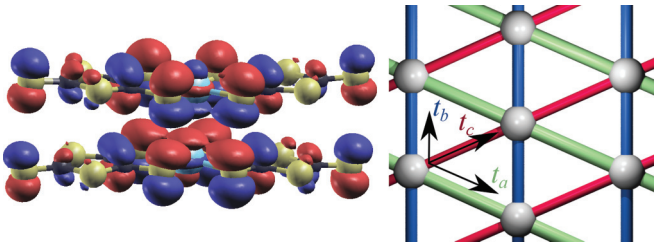

FIG. 4. (Color online) Left panel: Wannier orbital for the HOMO-ab bands of Sb-1. The antibonding HOMO character of the orbital is clearly visible. Right panel: The 2D tight-binding lattice generated in the a-b plane from the Wannier orbital of the left panel. Each gray point of the lattice represents a dimer. The widths of the various cylinders in the lattice are linearly proportional to the magnitude of the corresponding t (see Table I).

show one of the Wannier orbitals for these bands, clearly showing their HOMO-ab character [the other Wannier orbital is the same but in the other layer of $Pd(dmit)_2$ molecules]. Table I shows the three t's in the first-nearest-neighbor shell (see Fig. 4) computed from the HOMO-ab Wannier orbitals of several X-n systems (note that including more neighbors explicitly has no effect on these parameters, unlike in a band-fitting computation). These results are consistent with those found in past work.[20–22]

With the t's obtained from the Wannier orbitals, we can now explore the Hubbard model for Sb-1 with VMC. We find that the spiral magnetic state $|\mathrm{SP}\rangle$ has optimal pitch angles $\theta = 7\pi/9, \theta' = 3\pi/9$, that are commensurate to an 18×18 lattice size. The BCS wave function has finite pairing fields for $U/t_a > 6.75$ (i.e., when the system is insulating) and they are highly anisotropic: with the largest component along the t_a direction, the t_b component approximately half as large and with opposite sign, and the t_c component nearly zero. Figure 5 shows the optimized energies of these two wave functions as a function of U/t_a; $|\Psi_{\mathrm{SP}}\rangle$ is favorable for $6.75 < U/t_a < 11$, and $|\Psi_{\mathrm{BCS}}\rangle$ is favorable outside of this region.

The charge gap, G, can be calculated from the static structure factor, $N(q)$, by assuming that the low-momentum excitations are collective modes.[12,27] With this approximation, one finds that $G \propto \lim_{q\to 0} \frac{q^2}{N(q)}$, where $N(q) = \langle n_{-q} n_q \rangle$ and $n_q = 1/\sqrt{L} \sum_{r,\sigma} e^{iqr} n_{r,\sigma}$. As such, the metallic phase is characterized by $N(q)/q \to$ const as $q \to 0$, implying a vanishing gap at $q = 0$, and the insulating phase is characterized by $N(q)/q \to 0$ as $q \to 0$, implying a finite gap. Figure 5 shows

TABLE I. Comparison of the sets of one orbital model parameters for several X-n systems. All energies are given in meV. Starred references did not include H coordinates, so they were inserted manually. All structures used here were obtained at room temperature, except for Sb-1, which was obtained at 4 K.

X-n	μ	t_b	t_a	t_c	Ref.
N-0	34.8	44.3	48.6	38.9	23*
As-0	28.6	44.5	55.6	32.6	23*
P-1	29.3	39.8	48.4	46.4	24
Sb-1	32.3	46.9	56.5	39.8	25
Sb-2	32.4	35.2	45.5	44.1	26*

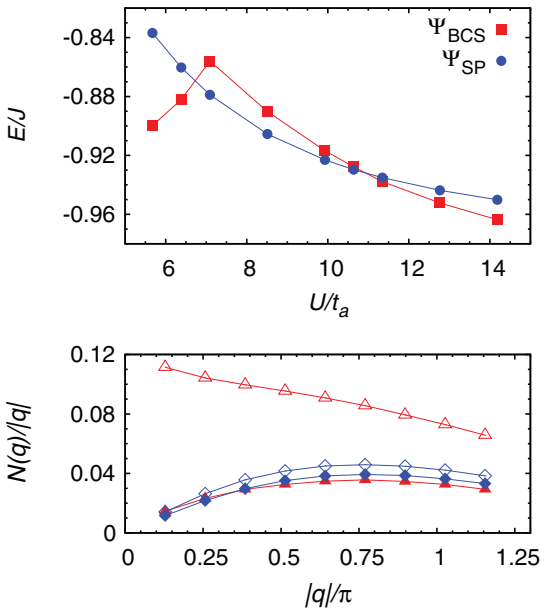

FIG. 5. (Color online) Upper panel: Variational energies per site for the FATL model with the parameters for Sb-1, by using the paramagnetic state (red squares), $|\Psi_{BCS}\rangle$, and the magnetic spiral state (blue circles), $|\Psi_{SP}\rangle$, as a function of U/t_a and in units of $J = 4t_a^2/U$. Both wave functions were computed on a $L = 324$ lattice, for which the optimal pitch angles ($\theta = 7\pi/9, \theta' = 3\pi/9$) are commensurate. Lower panel: $N(q)/q$ at $U/t_a = 6.4$ by using $|\Psi_{BCS}\rangle$ (empty triangles) and $|\Psi_{SP}\rangle$ (empty diamonds) and at $U/t_a = 7.1$ by using $|\Psi_{BCS}\rangle$ (full triangles) and $|\Psi_{SP}\rangle$ (full diamonds). Data show the metal to insulator transition in $|\Psi_{BCS}\rangle$, while the magnetic state is always insulating. Plots are presented along the line connecting the point $Q = (\pi, \pi/\sqrt{3})$ to the point $\Gamma = (0,0)$ in reciprocal space.

$N(q)/q$ versus q for the $|\Psi_{BCS}\rangle$ and $|\Psi_{SP}\rangle$ states at $U/t_a = 6.4$ and 7.1; either side of the point at which the $|\Psi_{SP}\rangle$ state becomes favorable. While the spiral magnetic $|\Psi_{SP}\rangle$ state is insulating on both sides of the transition, the $|\Psi_{BCS}\rangle$ state changes from metallic to insulating. Thus, we clearly see this is the metal-insulator transition (MIT). By examining $N(q)/q$, we confirm that the $|\Psi_{BCS}\rangle$ state remains insulating all the way above the MIT, in particular in the region $U/t_a > 11$, where it becomes favorable.

We note that an existing calculation of the interaction parameters using the constrained random-phase approximation finds $U/t_a \sim 11$ for Sb-1, in good agreement with our results for the location of the spin-liquid region.[21]

B. $t - t'$ model vs FATL

$Pd(dmit)_2$ systems are often represented by a $t - t'$ model, despite this symmetry not being found in the various t estimates, including our estimate in Table I.[20–22] Here we compare model results using the $t - t'$ approximation with a fully anisotropic triangular lattice (FATL) model, focusing our discussion on the spin-liquid candidate Sb-1. If we average the two larger t's of Sb-1, assuming $t = (t_a + t_b)/2$ and $t' = t_c$, we find that the equivalent $t - t'$ model has $t'/t = 0.77$. This model has been previously studied with variational Monte Carlo,[15] where for this value of t'/t the critical U for the spin-liquid transition is located at $U/t \sim 22$, while for the FATL this value is strongly reduced to $U/t_a \sim 11$. On the other hand, the metal-insulator transition is only slightly affected, raising from $U_c/t \sim 6$ for the $t - t'$ model to $U_c/t_a \sim 6.75$ for the FATL. These results are illustrated in the phase diagram in Fig. 6.

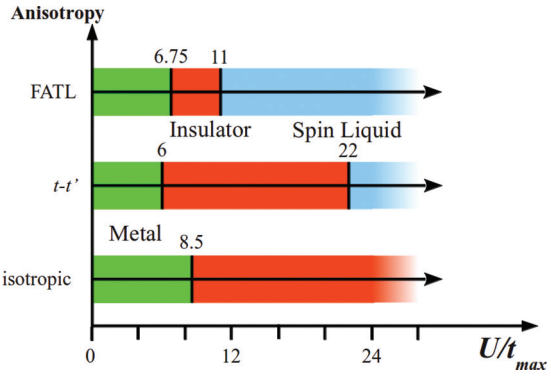

FIG. 6. (Color online) Phase diagram vs U/t_{max}, where t_{max} is the biggest hopping parameter in the model, for the isotropic, $t - t'$, and FATL models for Sb-1, showing the metallic (green), spiral ordered magnetic insulator (orange), and spin-liquid (cyan) phases. The spin-liquid phase is strongly enhanced by including the full anisotropy of the system, while the metal-insulator transition is only slightly changed.

We would like to point out that if we repeat our calculation for the P-1 system (which is almost truly $t - t'$) we find that in both the FATL and in the $t - t'$ model the transition to spin liquid occurs at $U/t_{max} \sim 13$, (where t_{max} is the biggest hopping parameter). Thus the enhancement of the spin-liquid phase is driven by anisotropy.

Interestingly, if we allow the pairing fields to be complex, we find that finite imaginary components lower the energy of the $|\Psi_{BCS}\rangle$ state slightly. This imaginary component appears for $U/t_a > 11$, the same point where the $|\Psi_{BCS}\rangle$ state becomes favorable again, and this seems to be due to the anisotropy of the system; indeed, by considering the less anisotropic P-1 system, we find a smaller imaginary component, while it is not seen in $t - t'$ models.

IV. CONCLUSIONS

We have shown that the high anisotropy in $Pd(dmit)_2$ materials can have important effects on the physics. Our electronic structure calculations find a range of different hopping parameters in good agreement with previous density-functional theory calculations. Relative to a $t - t'$, using a FATL model for Sb-1 increases the critical U for the metal-insulator transition only by ~10%, while it *halves* the critical U for the spin-liquid transition. With this reduction, existing parametrizations of Sb-1 place it in the spin-liquid regime. In addition, the spin-liquid phase develops a complex pairing function as it becomes favorable for $U/t_a > 11$, something not seen in the $t - t'$ model.

ACKNOWLEDGMENTS

We would like to acknowledge useful discussions with D. Cocks, C. Gros, M. Imada, and H. Seo; and H. Feldner for providing the H.F. code. We acknowledge the support of the German Science Foundation through Grant No. SFB/TR49.

[1]In the acceptor molecule, dmit stands for 1,3-dithiole-2-thione-4,5-dithiolate. The cation contains a pnictogen $X = \mathrm{N}$, P, As, Sb surrounded by methyl (Me, CH_3–) and ethyl (Et, C_2H_5–) groups. For details see K. Kanoda and R. Kato, Ann. Rev. Condens. Matter Phys. **2**, 167 (2011), and references therein.

[2]A. Kobayashi, H. Kobayashi, A. Miyamoto, R. Kato, R. A. Clark, and A. E. Underhill, Chem. Lett. **20**, 2163 (1991).

[3]K. Seya, Y. Kobayashi, T. Nakamura, T. Takahashi, Y. Osako, H. Kobayashi, R. Kato, A. Kobayashi, and H. Iguchi, Synth. Met. **70**, 1043 (1995).

[4]M. Tamura and R. Kato, J. Phys.: Condens. Matter **14**, L729 (2002).

[5]T. Itou, A. Oyamada, S. Maegawa, M. Tamura, and R. Kato, Phys. Rev. B **77**, 104413 (2008).

[6]B. J. Powell and R. H. McKenzie, Rep. Prog. Phys. **74**, 056501 (2011).

[7]P. Hauke, Phys. Rev. B **87**, 014415 (2013).

[8]K. Koepernik and H. Eschrig, Phys. Rev. B **59**, 1743 (1999).

[9]J. P. Perdew, K. Burke, and M. Ernzerhof, Phys. Rev. Lett. **77**, 3865 (1996).

[10]H. Eschrig and K. Koepernik, Phys. Rev. B **80**, 104503 (2009).

[11]A. C. Jacko, H. Feldner, E. Rose, F. Lissner, M. Dressel, R. Valentí, and H. O. Jeschke, Phys. Rev. B **87**, 155139 (2013).

[12]L. F. Tocchio, F. Becca, and C. Gros, Phys. Rev. B **83**, 195138 (2011).

[13]Z. Weihong, R. H. McKenzie, and R. R. P. Singh, Phys. Rev. B **59**, 14367 (1999).

[14]H. R. Krishnamurthy, C. Jayaprakash, S. Sarker, and W. Wenzel, Phys. Rev. Lett. **64**, 950 (1990).

[15]L. F. Tocchio, H. Feldner, F. Becca, R. Valentí, and C. Gros, Phys. Rev. B **87**, 035143 (2013).

[16]F. Franjic and S. Sorella, Prog. Theor. Phys. **97**, 399 (1997).

[17]F. Zhang, C. Gros, T. Rice, and H. Shiba, Supercond. Sci. Technol. **1**, 36 (1988).

[18]B. Edegger, V. Muthukumar, and C. Gros, Adv. Phys. **56**, 927 (2007).

[19]M. Capello, F. Becca, M. Fabrizio, S. Sorella, and E. Tosatti, Phys. Rev. Lett. **94**, 026406 (2005).

[20]E. P. Scriven and B. J. Powell, Phys. Rev. Lett. **109**, 097206 (2012).

[21]K. Nakamura, Y. Yoshimoto, and M. Imada, Phys. Rev. B **86**, 205117 (2012).

[22]T. Tsumuraya, H. Seo, M. Tsuchiizu, R. Kato, and T. Miyazaki, J. Phys. Soc. Jpn. **82**, 033709 (2013).

[23]A. Kobayashi, H. Kim, Y. Sasaki, K. Murata, R. Kato, and H. Kobayashi, J. Chem. Soc. Faraday Trans. **86**, 361 (1990).

[24]R. Kato, A. Tajima, A. Nakao, and M. Tamura, J. Am. Chem. Soc. **128**, 10016 (2006).

[25]R. Kato (private communication).

[26]A. Nakao and R. Kato, J. Phys. Soc. Jpn. **74**, 2754 (2005).

[27]R. P. Feynman, Phys. Rev. **94**, 262 (1954).